Vision Research 50 (2010) 271–278

Contents lists available at ScienceDirect

Vision Research

journal homepage: www.elsevier.com/locate/visres

Extending the eXpanded Nystagmus Acuity Function for vertical and multiplanar data

J.B. Jacobs [a,b,*], L.F. Dell'Osso [a,b,c]

[a] Daroff-Dell'Osso Ocular Motility Laboratory, Louis Stokes Cleveland Department of Veterans Affairs Medical Center and CASE Medical School, Cleveland, OH, USA
[b] Department of Neurology, Case Western Reserve University and University Hospitals Case Medical Center, Cleveland, OH, USA
[c] Department of Biomedical Engineering, Case Western Reserve University and University Hospitals Case Medical Center, Cleveland, OH, USA

ARTICLE INFO

Article history:
Received 11 February 2009
Received in revised form 29 May 2009

Keywords:
Eye movements
Nystagmus
Visual acuity
Foveation

ABSTRACT

We updated and extended the functionality of the eXpanded Nystagmus Acuity Function (NAFX), for application under more diverse circumstances, improving its clinical predictive value. The original NAFX "τ-surface" of minimum-necessary-foveation times had been individually calculated for each combination of position and velocity limits. We have replaced it with an idealized mathematical function that repairs the irregularities in its surface due to idiosyncrasies in the subject data used for the initial calculations. To extend applicability to multiplanar data, we combine horizontal and vertical eye-movement data into a single waveform using vector summation. Torsional eye movements have little effect on visual acuity and are ignored. Age-related visual acuity relationships, derived from population data, more accurately relate the NAFX value to acuity for individual patients. Using the same patient fixation data that established the original NAF and NAFX functions, we verified that the updated NAFX yielded equivalent results for uniplanar data. For biplanar data, the results were also comparable to those of uniplanar data of the same magnitude. The updated NAFX yields greater accuracy in prediction of potential visual acuity for subjects of all ages, for uniplanar and multiplanar nystagmus, extending the objective, direct measure of post-therapy waveform improvement, allowing selection of the best therapy for a wider range of nystagmus patients.

1. Introduction

The original eXpanded Nystagmus Acuity Function (NAFX) (Dell'Osso & Jacobs, 2002), which was based upon the Nystagmus Acuity Function (NAF) (Sheth, Dell'Osso, Leigh, Van Doren, & Peckham, 1995), is a mathematically derived relationship that predicts best potential visual acuity based on the attempts at foveation that occur within nystagmus waveforms. The calculations are based on the duration and repeatable cycle-to-cycle stability of these foveation periods, yielding a numerical result that is linearly related to Snellen/decimal acuity.

The "foveation window," which determines the time points during which visual input may be expected to contribute towards best acuity, is a two-dimensional construct, with position and velocity error constraints that must be satisfied simultaneously. As the target falls further from the center of the fovea, receptor density (i.e., detail sensitivity) decreases approximately exponentially (Curcio, Sloan, Kalina, & Hendrickson, 1990; Curcio, Sloan, Packer, Hendrickson, & Kalina, 1987); likewise, the faster the target is moving across the fovea (regardless of whether it is the eye or the target that is moving), the more vision is degraded (Chung & Bedell, 1996; Westheimer & McKee, 1975).

In the original NAF, these limits were strictly restricted to a position error of no more than ±0.5° (the effective foveal radius), and a slip velocity of no more than ±4.0°/s, sufficient to allow accurate acuity assessment of many of the INS patients we evaluated. However there remained other patients with ocular motor instabilities so severe that they could not meet these criteria, preventing the analysis of their nystagmus with this function. This prompted us to develop the NAFX, which allows for larger foveation windows (up to ±6° by ±10°/s) by varying τ (tau), the time constant for foveation duration, based on normative data (Sheth et al., 1995). A complete description of the methods used to expand the NAF into the NAFX, and the rules for its application in the analysis of nystagmus data can be found elsewhere (Dell'Osso, 2005; Dell'Osso & Jacobs, 2002).

The collection of τ for all combinations of position and velocity limits is called the "τ-surface," and is shown in Fig. 1a. While it is, in general, a regular-appearing shape, there are obvious irregularities in the surface, most notably along the lower position values (left side of Fig. 1). These distortions are a consequence of some of the data that were used to generate the original surface: while

* Corresponding author. Address: Daroff-Dell'Osso Ocular Motility Laboratory, Louis Stokes Cleveland Veterans Affairs Medical Center, 10701 East Boulevard, Cleveland, OH 44106, USA. Fax: +1 216 231 3461.
E-mail address: jx24@case.edu (J.B. Jacobs).
URL: http://www.omlab.org (J.B. Jacobs).

0042-6989/$ - see front matter © 2010 Published by Elsevier Ltd.
doi:10.1016/j.visres.2009.05.019

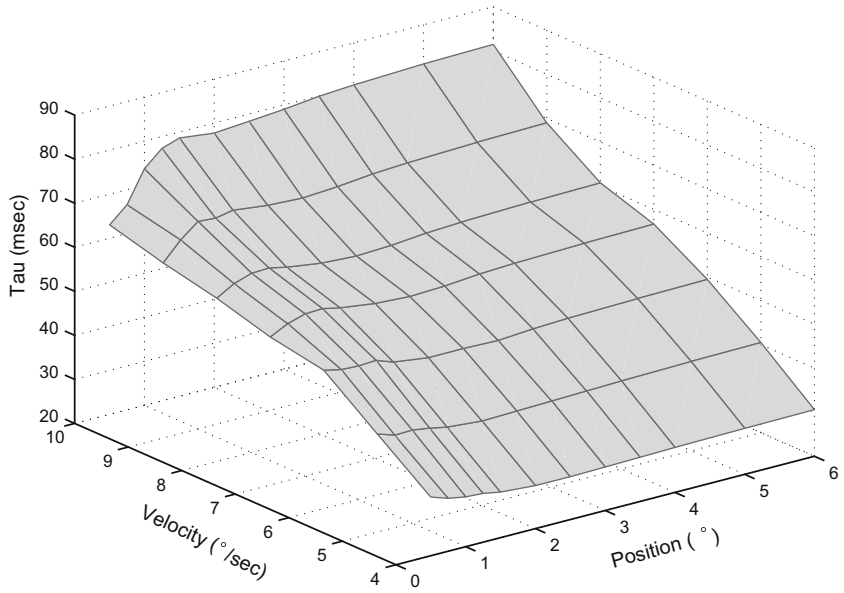

Fig. 1. The original τ-surface, generated from multiple data sets from individuals with INS, and used in the software for the first version of the NAFX function. Note the unevenness of the surface caused artifacts in selection and evaluation of the data.

jerk with extended foveation (J_{ef}) waveform data has only one foveation period per cycle, we also used data containing the pseudopendular with foveating saccades (PP_{fs}) waveform, which has two, with one following the foveating saccade, and a second, usually briefer, period following the braking saccade (Jacobs, Dell'Osso, & Leigh, 2003). During lower-amplitude PP_{fs} analysis, as the position limit was increased, the slow phase following the braking saccade was inadvertently included in the calculation in addition to the intended period following the foveating saccade, resulting in a greater measure of foveation time. As a result, the time necessary to yield the equivalent acuity was calculated to be lower than its true value. The first of our goals was the refinement of the τ-surface.

Our second goal was to expand the utility of the NAFX to allow analysis of patients whose nystagmus is not limited to a single dimension. As originally developed, the NAFX was applied only to nystagmus that occurred within one plane, as most INS is predominantly horizontal. However, there are a number of subjects who have a vertical element to their INS, and in some cases its magnitude can be larger than the horizontal component. It is even possible to see INS that is purely vertical, though this is quite rare. There is no reason why the algorithm cannot be used to evaluate data in the vertical plane as well, if we make the assumption—consistent with two-dimensional maps of photoreceptor distribution around the fovea—that vertical movement degrades visual perception in a manner equivalent to horizontal oscillations used to develop the original NAF, though we have not yet encountered a sufficient number of subjects with purely vertical INS to verify the results. While it is also possible that there are differences in processing horizontal and vertical movement that lead to different degradation of perception, we have based our calculations on equal effects. These caveats noted, we further propose that the NAFX should be suitable for analysis of multiplanar nystagmus waveforms as one operation, i.e., by first combining the separate horizontal and vertical components into a resultant vector by way of a simple mathematical transform. This transformation is an approximate mapping, as we attempt to compress two spatial dimensions into one without too much loss of information (see "Methods" for details).

We are ignoring the known, small torsional components of INS, even though they are frequently present as the consequence of simple mechanical interactions ("crosstalk") of the extraocular muscles (Averbuch-Heller, Dell'Osso, Leigh, Jacobs, & Stahl, 2002). We believe this to be a valid simplification as the torsional magnitudes are almost uniformly quite small (under 5°) and no matter what the magnitude, the target remains within the fovea despite the torsion during the foveation periods (based on the assumption that the axis of rotation for torsional movements passes through the center of the fovea). Furthermore, visual perception is most likely relatively insensitive to torsional movements that fall within this limit (Kushner, 2004).

A final goal driving this study were improvements to the software suite (OMtools) we developed to facilitate exploration of eye-movement data and performance of the analysis. As it is intended for use by clinicians and researchers who are not necessarily programmers, it must have a *user-friendly* interface that allows for ease-of-use. This includes presentation of data in an intuitive manner as well as the automation of some of the simple repetitive, yet time-consuming and error-prone tasks required to perform an analysis, while retaining the ability to allow deeper investigation of the data being analyzed.

2. Methods

2.1. Eye-movement recording

The eye-movement recordings used for analysis were made over the space of several years, using a variety of techniques. Purely horizontal eye-movement recordings were made using infrared reflection (Applied Scientific Laboratories, Waltham, MA) that was linear to ±20° and monotonic to ±25–30° with a sensitivity of 0.25°. Biplanar data were recorded using either scleral coil or high-speed digital-video systems. The magnetic search-coil system (CNC Engineering, Seattle, WA) had a sensitivity of better than 1 arcmin, with linearity of one part in 14,014 and drift of 0.2–0.3 arcmin/h. Noise was less than 2 arcmin and eye position was stored to the nearest arcmin. The digital-video system (EyeLink II, SR Research, Mississauga, ON, Canada) had a linear range of ±30° horizontally and ±20° vertically with a gaze position accuracy error of under 0.5° on average.

Regardless of recording technique, each eye was calibrated under monocular viewing conditions, with the fellow eye behind cover, to obtain accurate position information and to document small tropias and phorias that might otherwise be hidden by the nystagmus. Monocular calibration is critical to determining which eye is fixating and identifying when the fixating eye switches; the NAFX can be related to visual acuity only when calculated using data from the fixating eye. Eye positions and velocities (obtained by analog differentiation of the position channels) were displayed on a strip-chart recording system (Beckman Type R612 Dynograph) to maintain a continuous running record of the experimental sessions.

All data were sampled with 16-bit resolution. The IR, digital-video and some of the search-coil data were sampled at 500 Hz, while the rest of the search-coil data were sampled at 488 Hz. Only position data were recorded directly; velocity information was obtained *post hoc* by differentiation of position using a central-point differentiator, which is mathematically equivalent to an ideal differentiator followed by a low-pass filter. This method does not lead to significant distortion of the velocity waveform, as the 3 dB bandwidth for data sampled at 500 Hz, filtered with $n = 2$ is 55.37 Hz (Bahill & McDonald, 1983), well above the frequencies where the majority of spectral energy is concentrated for the nystagmus waveforms we were studying (Jacobs, Dell'Osso, & Leigh, 2003).

2.2. Protocol

Written consent was obtained from subjects before the testing. All test procedures were carefully explained to the subject before the experiment began, and were reinforced with verbal commands during the trials. Subjects were seated in a chair with headrest and either a bite board or a chin stabilizer 57 in. from an arc of red LEDs, far enough to minimize convergence effects. At this distance the LED subtended less than 0.1° of visual angle. The room light could be adjusted from dim down to blackout to minimize extraneous visual stimuli. An experiment consisted of from one to ten trials, each lasting under a minute with time allowed between trials for the subject to rest. Trials were kept this short to guard against boredom because CN intensity is known to decrease with inattention.

2.3. Modified τ-surface

To calculate the updated τ-surface based on the original data, we elected to reconstruct it by modifying its irregular values. To do this we took each curve of fixed velocity for each position limit and (using the MATLAB curve-fitting toolbox, The Mathworks, Natick, MA) performed a curve fit of the form $ae^{bx} + ce^{dx}$ to the non-outlier points. We selected this exponential function because the original NAFX (and the NAF from which it was derived) is based on an exponential relationship for determining necessary foveation times; we therefore reasoned that our expansions of the velocity and position criteria would likely follow this relation as well. The newly fit curves were assembled into a new surface and adjusted to match pre-defined borders as described in the Section 3.

2.4. Vector calculation

In converting the independent horizontal and vertical eye-movement waveforms to a single resultant waveform we are attempting to map two spatial dimensions into one, yet retain all the information of those two dimensions while presenting them in a meaningful way. We started by applying a simple vector summation of the form $r = (x^2 + y^2)^{1/2}$. This by itself, however, results in a purely positive one-dimensional vector (e.g., all "rightward" and/or "upward"), which may grossly distort the original nystagmus waveform resulting in two undesired consequences: it decreases the effectiveness of an investigator's ability to identify nystagmus waveforms and interpret the subject's behavior. Furthermore, this operation destroys information, e.g., the true distance between successive foveation periods, or the peak-to-peak amplitude of the oscillations, which were carried in the angular relationships of a true radial (r, θ) plot vs. time. One solution would be to modify (recode and extensively test) all existing analysis programs to work with radial coordinates, instead of Cartesian coordinates, which would guarantee mathematical exactness, though it would still deprive the investigators of their experience interpreting eye-movement recordings. We are investigating this approach on a parallel track. However, for this study we opted to use a compromise: we still "flatten" two spatial dimensions into one, but we retain the direction information contained in the major nystagmus component and reapply it to the new vector. For INS, the dominant component will almost always be the horizontal movement. The reasoning behind this method is illustrated in Fig. 2, which shows (a) the separate horizontal and vertical components; (b) a 3-Dimensional plot of the horizontal and vertical components; (c) viewed end on as a nystagmus scanpath (horizontal vs. vertical); and (d) the resultant vector created using our methods with major (horizontal) component direction mostly preserved. It is this vector that is then analyzed using the NAFX. In a case where the dominant component switched between planes, we performed the operation piecewise on the individual segments, assigning the direction according to the major component for each segment, and then rejoining them into the full record.

3. Results

3.1. Calculating the modified τ-surface

By examining the data from the original τ-surface for variable position limits along the fixed-velocity-limit curves, we could easily see the errors due to including in our calculations the foveations that followed the braking saccades in addition to the ones that followed the foveating saccades. These errors occurred for position limits less than 2°, and were more apparent for the lower velocity curves, as shown in Fig. 3. The open circles represent the original τ values, and the solid lines the results of applying the exponential fit to the non-outlier data. The resulting curves all had r-squared values of no less than 0.95, and several were as good as 0.99+. Note that the lower velocity curves become more and more linear, as do the higher position portions of all the curves. The border for 4°/s was defined to be linear with a constant value of 33 ms, i.e., the unmodified τ value from the original NAF equation. Fig. 4a shows the surface plot constructed using only the new velocity curves. While the surface is now much more regular, it still has irregular dips and rises, most noticeable when viewing the upper position border, i.e., all velocities for position =6.0°. We smoothed these out by calculating a strictly linear fit for that curve (r-squared value = 0.986), with the velocity = 4.0°/s value shifted to match the above-defined value of 33 ms. We then shifted the end points for the other fixed-velocity-limit curves to lie along this line. The result of this adjustment is the final τ-surface as presented in Fig. 4b.

Fig. 5a shows the original and modified τ-surfaces superimposed for comparison. The overall differences between the two surfaces are generally quite small, averaging 2 ms overall, and no more than 5.1 ms in the worst case. The difference expressed as a percentage between the original and the modified τ-surfaces is plotted in Fig. 5b. The mean across the absolute value of all errors was 2.17%, with a maximum error approaching 8% in only a few locations.

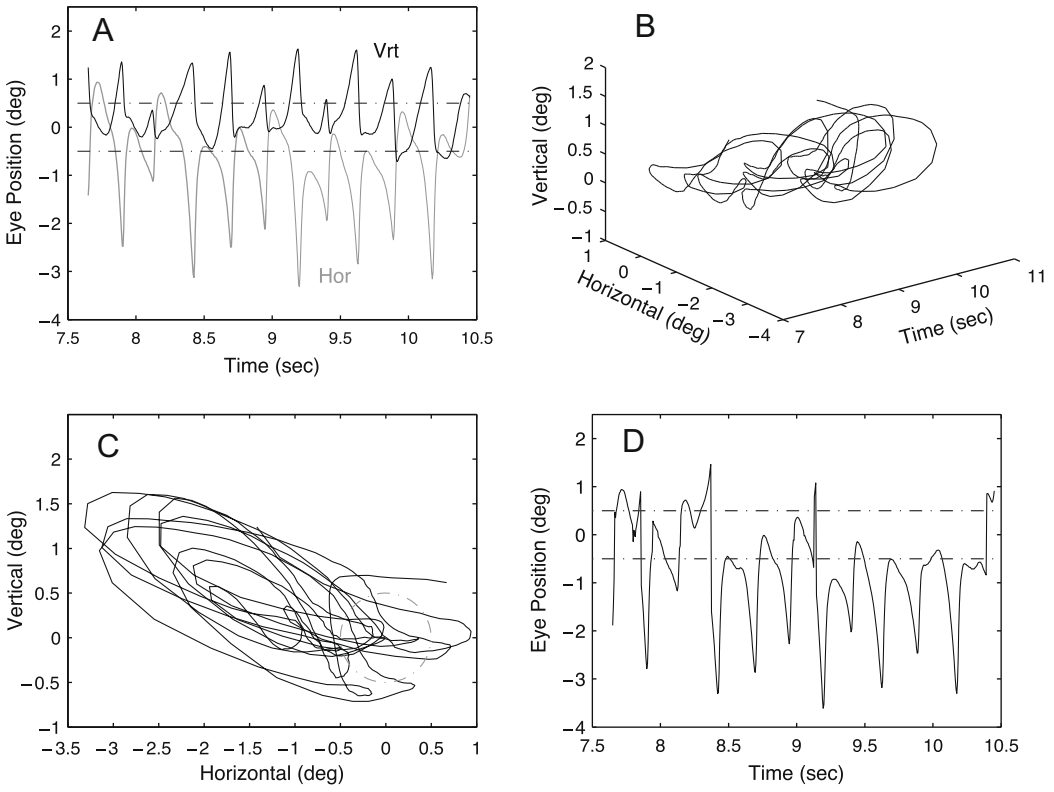

Fig. 2. (A) Horizontal and vertical eye-movement data. (B) 3-dimensional plot (horizontal, vertical vs. time) renders nystagmus waveforms unrecognizable. (C) Viewed along the time axis reduces to a nystagmus scanpath (horizontal vs. vertical). (D) Simplified resultant vector created using the technique discussed above. The dashed lines at ±0.5° represent the foveal extent.

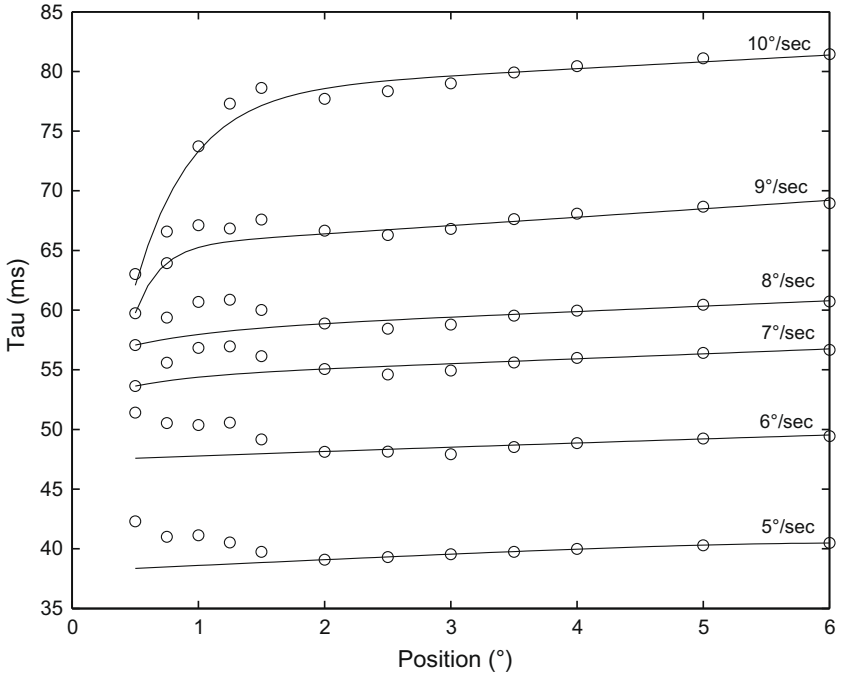

Fig. 3. The individual fixed-velocity curve fits. Open circles represent the values from the original tau-surface, solid lines show the resulting double-exponentials.

3.2. Using the modified τ-surface

We tested the new surface by reevaluating NAFX calculations that had been performed over a variety of foveation-window position and velocity limits. We reran analyses of forty segments of previously examined subject data and compared the values obtained using the original and modified τ-surfaces. The results are shown in Fig. 6a. For each analysis, we plotted the value from $NAFX_{v1}$ along the x-axis, and from $NFAX_{v2}$ along the y-axis. Perfect equality would lie along the line $x = y$ (i.e., slope of 1.0).

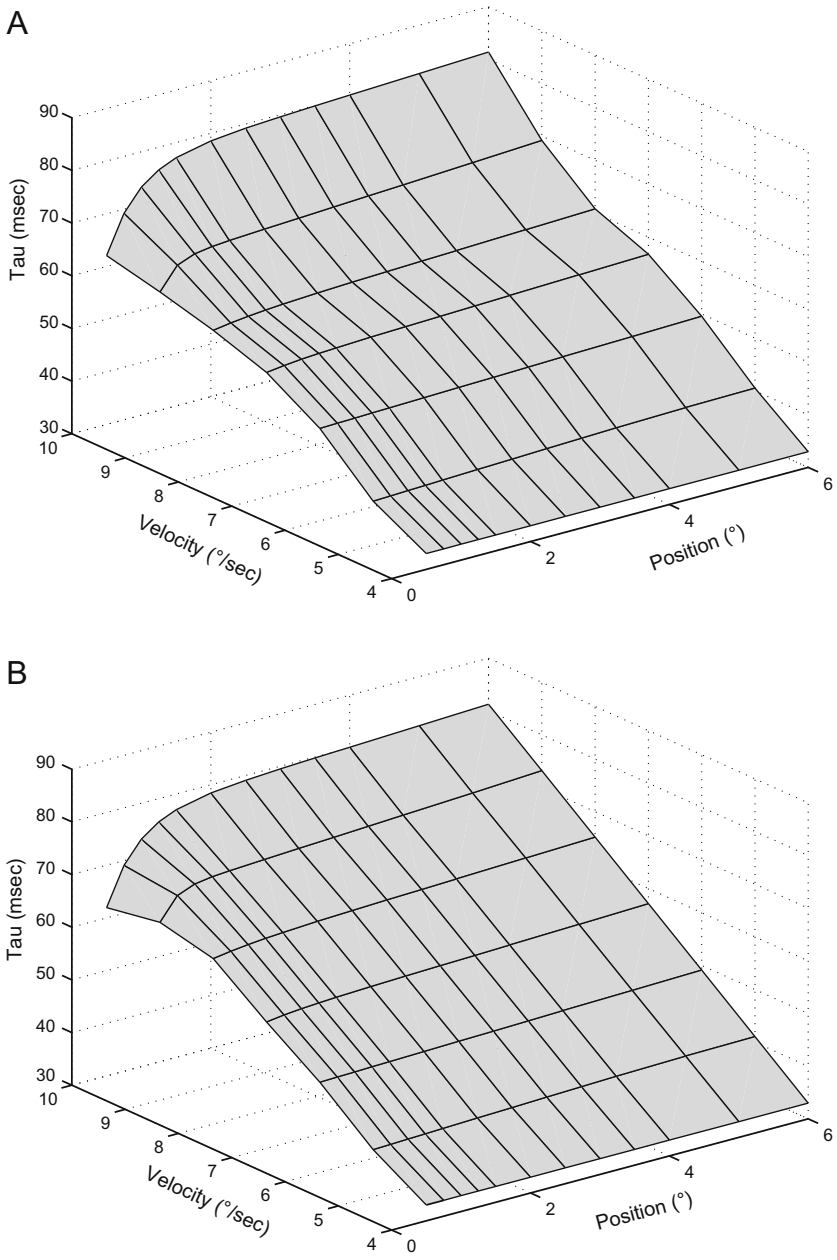

Fig. 4. (A) The modified τ-surface composed of the unshifted double-exponential curve fits. (B) Final surface following shifting of fixed-velocity curves to match the forced linear border at position = 6°.

A first-order fit gives a slope of 0.975 with an *r*-squared value of 0.99. The average absolute error was 1.2%, with a standard deviation of 1.6%, demonstrating that the two surfaces yield equivalent results, so the new function is in close agreement with the original. Furthermore, this good correspondence is not simply due to the majority of the analyses being performed in the minimally changed portion of the τ-surface. Fig. 6b shows another view of the results from the analyses, arranged by their position and velocity limits. Note that the heavy concentration of (*P*, *V*) pairs fall in the under -2° range, which was the portion of the old τ-surface with the greatest irregularities, due to double-counting foveations.

3.3. 2-Dimensional NAFX analyses

Refer back to Fig. 2, which shows the creation of a radial waveform from horizontal and vertical components. Here, the horizontal magnitude is approximately five times that of the vertical, and the resulting combined waveform remains recognizable as PP_{fs} with the same magnitude and foveation characteristics as the horizontal component, as shown by the resulting radial NAFX of 0.46, compared to 0.45 for the horizontal and 0.85 for the vertical. The NAFX analyses of 22 (horizontal, vertical and radial) triplets are plotted in Fig. 7. Most of the time, as expected, the radial result was nearly the same, or just slightly worse, than that of the component with the lower NAFX. However, on several occasions the radial analysis unexpectedly yielded a *better* result than the poorer component for reasons that we will discuss below.

3.4. Usability improvements

In addition to the original command-line interface (CLI), a graphical user interface (GUI) was added to the NAFX allowing it

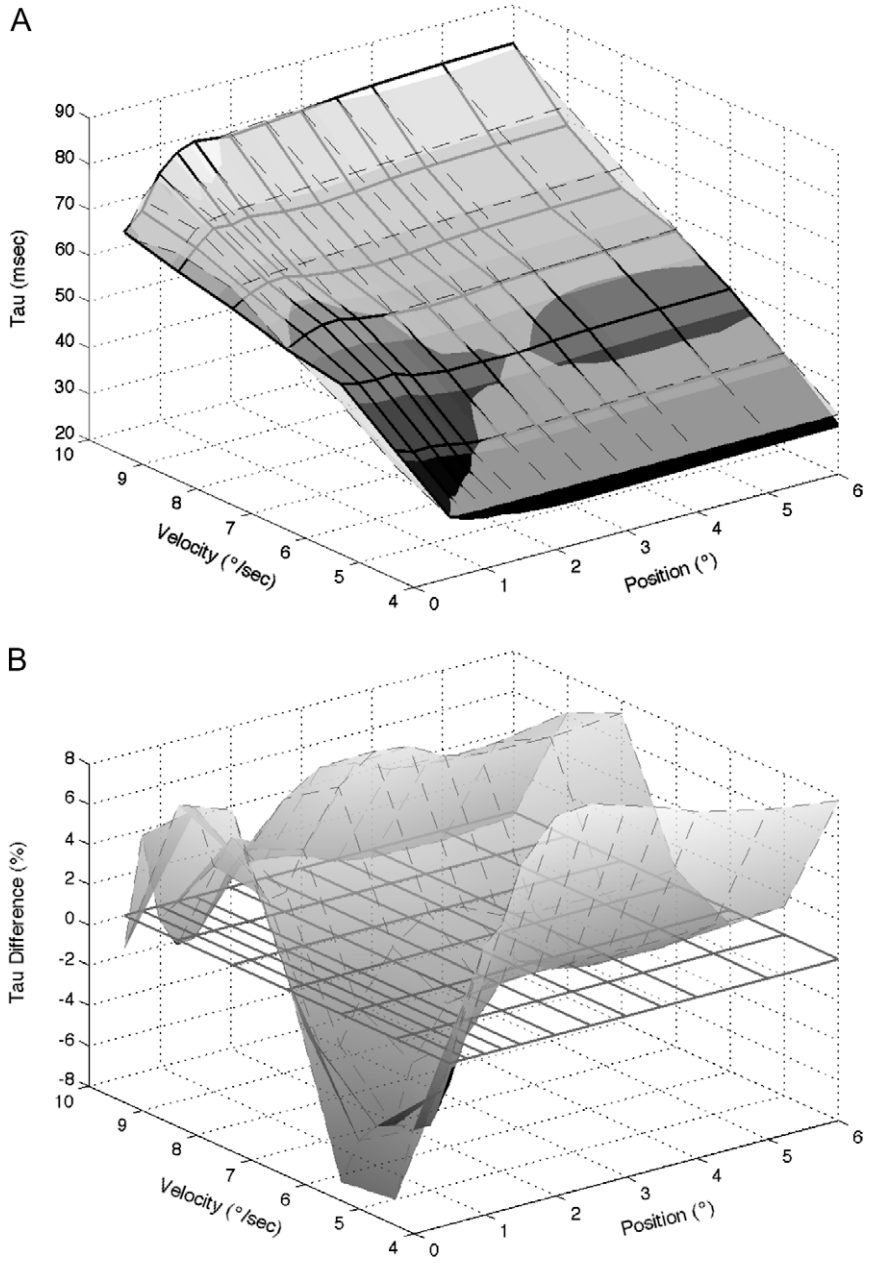

Fig. 5. The difference between the original and modified τ-surfaces, (A) overlaid with the original surface rendered opaque and the revised surface rendered translucent, (B) plotted as a percentage difference. The heavy dark grid is the zero-difference plane, shown for reference.

to be used interactively or in batch mode. The GUI mode produces a CLI-equivalent output, allowing for a "paper trail" so analyses can easily be stored in a text file, re-run, and even modified as necessary. Because visual acuity in humans exhibits age sensitivity (Westheimer, 2003; Westheimer & McKee, 1975), the subject's age may be selected from a menu of ranges for an accurate NAFX-to-Snellen conversion. The 'NAFX prep' function automates much of the procedure, allowing for rapid selection and evaluation of data segments (position and velocity sub-array creation and naming, and position-shifting for foveation) for calculation of the NAFX value. As part of generating the velocity arrays, automatic low-pass filtering (~0.05 of sampling frequency, e.g., ~25 Hz for 500 Hz sampled data) is included that matches the manually filtered position arrays. The NAFX is then calculated using either the number of foveations as determined by the NAFX's 'detectfovs' algorithm, or a user-determined number based on the graphical outputs of the 'NAFX prep' function (for examples, see the on line tutorial, including illustrations of the GUI) (Dell'Osso, 2005). These additions all contribute to a general ease-of-use (e.g., all parameters clearly identified and modifiable) that now facilitates the use of the NAFX for analysis of foveation quality in subjects with nystagmus.

4. Discussion

The original NAFX has demonstrated its utility as a method to predict best potential visual acuity based solely on waveform and foveation characteristics (Hertle, Anninger, Yang, Shatnawi, & Hill, 2004; Jacobs, Dell'Osso, Wang, Bennett, & Acland, 2005; Sarvananthan, Proudlock, Choudhuri, Dua, & Gottlob, 2006). In fact, all other data points from the nystagmus waveforms are discarded by the algorithm. Thus, nystagmus amplitude, fast phases, and the

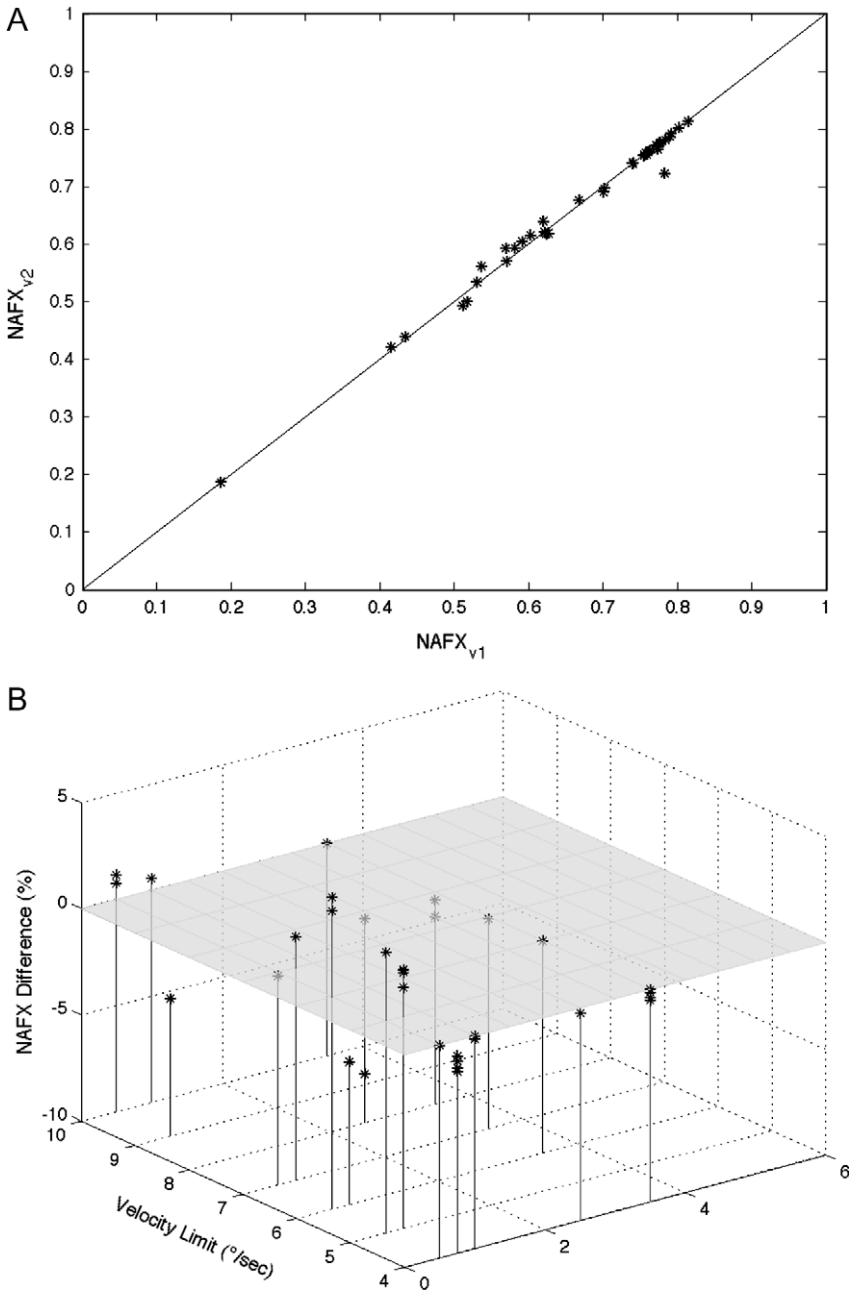

Fig. 6. Comparison of 40 NAFX analyses using both the original τ-surface (x-coordinate) and modified τ-surface (y-coordinate). (A) The line at 45° represents equivalent results for both methods. (B) The same analysis results arranged by position and velocity window limits and shown as percentage difference.

non-contributing remainder of the slow-phase waveform play no part in determining visual acuity.

Our current work has further enhanced its usefulness by: (1) removing minor irregularities in the τ-surface that is used to calculate the NAFX; (2) extending the algorithm to allow its application to multiplanar nystagmus analysis; and (3) adding improvements in interface and workflow to facilitate usability by a wider range of users.

We believe that our solution to the first issue, keeping the majority of the original surface and using curve fitting to correct particular sections, is a valid approach. As stated, the original surface has been shown to yield useable results, albeit with some minor caveats, based on known flaws in the original procedures and data used to calculate it. Since the errors in the surface were mostly confined to a limited region, and attributable to a specific cause, i.e., the failure to account for double foveations in the PP_{fs} waveforms that were used to generate it, we chose to carefully excise the inappropriate data points and generate new points by extrapolating from the reliable existing results. By careful examination of the irregularities it was possible to retain most of the τ-surface, rather than having to discard it and recalculate it in its entirety.

Why is the effect on τ of the position error more apparent for the lower velocity curves? The most probable explanation is that, for the same positions on the higher-velocity curves, the difference due to the increased velocity limit now plays a greater part, making the position-only increase a less significant contribution to the total τ. At 4.0°/s, the target spends sufficient "snapshot time" on the high-acuity portion of the fovea. Therefore, increasing the position window was not likely to add towards vision and we were able to force the 4.0°/s border to 33 ms over all positions. At the high end of the velocity window, we fit the original τ-surface data with a 6° line, again with little difference.

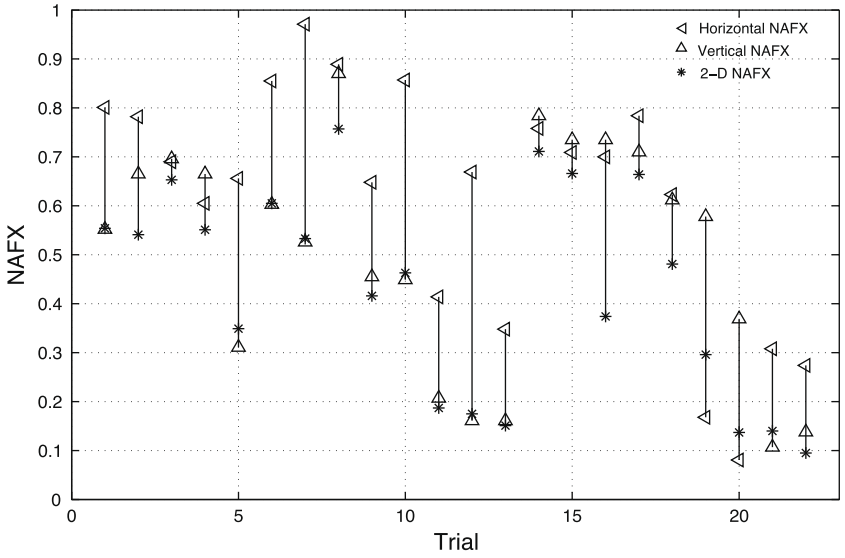

Fig. 7. The result of 22 biplanar NAFX analyses compared to analyses of the individual uniplanar components. In most, but not all cases, the radial NAFX is less than that of both individual components, as expected.

The worst-case differences between the original and revised surfaces are quite small, (under 8%, with an average difference of 2.17%), and calculations using both versions show comparable results, demonstrating that the updated τ-surface is a suitable replacement. These results also suggest that the NAFX is not as sensitive to minor variations in τ as it is to the selection of appropriate (i.e., not containing artifacts of recording, changes in the fixating eye, or inattention) data segments and foveation-window parameters. Built-in safeguards in the NAFX software provide warnings under some circumstances when these criteria are not met. The original procedures for the use of the NAFX that guarantee its relationship to visual acuity (Dell'Osso, 2005; Dell'Osso and Jacobs, 2002) remain unchanged by modifications implemented here.

The extension of the NAFX to multiple planes has proven to be a more complex problem that it first appeared. We have attempted to map a three-dimensional waveform (h, v vs. t) into two-dimensions (r vs. t) while remaining mathematically exact, which is not always possible. There are cases where the mapping will distort the resulting waveform so that, e.g., successive foveation periods will appear closer together than they really are, leading to a decreased standard deviation of foveation position, resulting in an artificially high NAFX. The other challenge is that we would like the resulting waveform to remain recognizable as a nystagmus waveform so that the investigator can use personal expertise to select appropriate segments of data for analysis and to guide (or override) the program's operations as necessary. Unfortunately, these two directives are often in conflict.

Finally, the introduction of an improved user interface simplifies operations and relieves the investigator of the highly repetitive and purely mechanical tasks required to prepare a segment of data for analysis. The resulting reduction in divided attention yields much faster performance, and facilitates exploration of the data by making it interactive in real time.

Acknowledgement

This research was supported by the Department of Veterans Affairs Merit Review.

References

Averbuch-Heller, L., Dell'Osso, L. F., Leigh, R. J., Jacobs, J. B., & Stahl, J. S. (2002). The torsional component of 'horizontal' congenital nystagmus. *Journal of Neuro-Ophthalmology, 22*(1), 22–32.

Bahill, A. T., & McDonald, J. D. (1983). Frequency limitations and optimal step size for the two-point central difference derivative algorithm with applications to human eye movement data. *IEEE Transactions on Biomedical Engineering, 30*(3), 191–194.

Chung, S. T., & Bedell, H. E. (1996). Velocity criteria for "foveation periods" determined from image motions simulating congenital nystagmus. *Ophthalmology and Visual Science, 73*(2), 92–103.

Curcio, C. A., Sloan, K. R., Kalina, R. E., & Hendrickson, A. E. (1990). Human photoreceptor topography. *Journal of Comparative Neurology, 292*(4), 497–523.

Curcio, C. A., Sloan, K. R., Jr., Packer, O., Hendrickson, A. E., & Kalina, R. E. (1987). Distribution of cones in human and monkey retina: Individual variability and radial asymmetry. *Science, 236*(4801), 579–582.

Dell'Osso, L. F. (2005). *Using the NAFX for eye-movement fixation data analysis and display*. OMLAB Report, #111005, pp. 1–7. <http://www.omlab.org/OMLAB_page/Teaching/teaching.html>.

Dell'Osso, L. F., & Jacobs, J. B. (2002). An expanded nystagmus acuity function: Intra- and intersubject prediction of best-corrected visual acuity. *Documenta Ophthalmologica, 104*, 249–276.

Hertle, R. W., Anninger, W., Yang, D., Shatnawi, R., & Hill, V. M. (2004). Effects of extraocular muscle surgery on 15 patients with oculo-cutaneous albinism (OCA) and infantile nystagmus syndrome (INS). *American Journal of Ophthalmology, 138*, 978–987.

Jacobs, J. B., Dell'Osso, L. F., & Leigh, R. J. (2003). Characteristics of braking saccades in congenital nystagmus. *Documenta Ophthalmologica, 107*, 137–154.

Jacobs, J. B., Dell'Osso, L. F., Wang, Z., Bennett, J., & Acland, G. M. (2005). *Using the NAFX to measure the effectiveness over time of gene therapy in canine LCA.* Annual Meeting Abstract and Program Planner [on CD-ROM or accessed at <www.arvo.org>]. p. ARVO Abstr 2401.

Kushner, B. J. (2004). Ocular torsion: Rotations around the "WHY" axis. *Journal of Aapos, 8*(1), 1–12.

Sarvananthan, N., Proudlock, F. A., Choudhuri, I., Dua, H., & Gottlob, I. (2006). Pharmacologic treatment of congenital nystagmus. *Archives of Ophthalmology, 124*(6), 916–918.

Sheth, N. V., Dell'Osso, L. F., Leigh, R. J., Van Doren, C. L., & Peckham, H. P. (1995). The effects of afferent stimulation on congenital nystagmus foveation periods. *Vision Research, 35*, 2371–2382.

Westheimer, G. (2003). Visual acuity. In P. L. Kaufman & A. Alm (Eds.), *Adler's physiology of the eye. Clinical application* (pp. 453–469). St. Louis: Mosby.

Westheimer, G., & McKee, S. D. (1975). Visual acuity in the presence of retinal-image motion. *Journal of the Optical Society of America, 65*, 847–850.